Electronic Supplementary Material (ESI) for Journal of Materials Chemistry A.

Supporting Information for

Microwave-assisted synthesis of black phosphorus quantum dots: efficient electrocatalyst for oxygen evolution reaction

Munkhbayar Batmunkh,[1]* Munkhshur Myekhlai,[2] Abdulaziz S. R. Bati,[1] Susanne Sahlos,[3] Ashley D. Slattery,[4] Tania M. Benedetti,[2] Vinicius R. Gonçales,[2] Christopher T. Gibson,[3,5] J. Justin Gooding,[2] Richard D. Tilley,[2] and Joseph G. Shapter,[1,3]*

[1] Australian Institute for Bioengineering and Nanotechnology, The University of Queensland, Brisbane, Queensland 4072, Australia.

[2] School of Chemistry, The University of New South Wales, Sydney, New South Wales 2052, Australia.

[3] Flinders Institute for NanoScale Science and Technology, College of Science and Engineering, Flinders University, Adelaide, South Australia 5042, Australia

[4] Adelaide Microscopy, The University of Adelaide, Adelaide, South Australia 5005, Australia

[5] Flinders Microscopy and Microanalysis, College of Science and Engineering, Flinders University, Adelaide, South Australia 5042, Australia

E-mail: m.batmunkh@uq.edu.au; j.shapter@uq.edu.au

Experimental

Materials

Unless otherwise stated, all chemicals and reagents were purchased from Sigma-Aldrich Co., Ltd., Australia. BP (99.998% pure) was purchased from Smart Elements.

Synthesis of BPQDs dispersion

Black phosphorus quantum dots (BPQDs) were produced in N-methyl-2-pyrrolidone (NMP) solvent using a microwave (MW)-assisted exfoliation method. In a typical experiment, black phosphorus (BP) crystals were ground and added into NMP solvent with a concentration of 5 mg mL^{-1}, followed by heating using the commercial microwave system (StartSYNTH Microwave Synthesis Labstation, Milestone s.r.l). We note that StartSYNTH Microwave Synthesis technique can operate at a maximum power of 600 W but the actual power applied is determined by the experimental parameters set. The exfoliation for the BP nanosheet preparation was performed at 50 ^{o}C temperature for 10 min, whilst the reaction for the BPQDs synthesis was carried out at 120 ^{o}C for 30 min. Then, a supernatant was taken and centrifuged at 6000 rpm for 30 min. Finally, the stable dispersion of BPQDs in NMP was collected.

Synthesis of CoO_x nanoparticles

CoO_x nanoparticles were prepared using an organic-phase solution seed mediated approach. Briefly, a solution containing 0.25 mmol cobalt (II) acetylacetonate as a precursor and 5 eq. mol of hexadecylamine as a surfactant were dissolved in mesitylene. The mixture was then reacted under 3 bar hydrogen at 140 ^{o}C for 24 h. After the reaction, H_2 was released and purification was carried out twice using toluene and ethanol solution (1:1 volume ratio) at 8000 rpm to obtain uniform CoO_x nanoparticles.

Preparation of working electrodes

All electrocatalysts (BPQDs, CoO_x and/or CoO_x-BPQDs) were immobilised on carbon powder as support for the electrocatalytic studies. For this purpose, a certain amount of electrocatalyst material and carbon black (Vulcan XC-72) (see Table S3 for detail) were suspended in toluene and the mixture was sonicated for 2 h to obtain a homogenous distribution. For the preparation of CoO_x-BPQDs/C, the BPQD dispersion was added into the CoO_x/C, followed by sonication. Then the solvents were removed from the carbon supported catalysts based dispersions by centrifuging and drying the samples. The elemental composition in the final composite is shown in the ICP-MS data (Table S3). The carbon loaded electrocatalysts were re-dispersed in isopropyl alcohol (IPA) to obtain 2.5 mg mL^{-1} ink. Then, 20 µL catalyst ink was deposited onto a glassy carbon rotating disk electrode (RDE).

Characterisation

Atomic force microscopy (AFM) was performed in air using a Bruker multimode 8 AFM with Nanoscope V controller, operating in standard tapping mode. The AFM probes used were silicon HQNSC15/AlBS Mikromasch probes (nominal tip diameter with spring constants of 16 nm and 40 N/m respectively). Set-point, scan rate and gain values were chosen to optimise image quality using procedures outlined by Nemes-Incze et al.[1] The AFM topography images have been flattened and nanoparticle height analysis measurements were made using the section analysis tool of Nanoscope Analysis 1.4. The AFM scanner was calibrated in X, Y and Z directions using silicon calibration grids (Bruker model numbers PG: 1 µm pitch, 110 nm depth and VGRP: 10 µm pitch, 180 nm depth).

Raman spectra were acquired using a Witec alpha300R Raman microscope at an excitation laser wavelength of 532 nm with a 100x objective (numerical aperture 0.9). Typical integration times for single Raman spectra were between 30-60 s for 2-3 accumulations. The highest resolution grating available on the instrument (1800 grooves mm^{-1}) was used. This grating has a spectral resolution of ~1 to 2 wavenumbers. Laser power levels were kept as low as possible to prevent sample damage.[2] The power was approximately 1 mW or below.

The optical absorption of the BPQD dispersion was examined using a UV-vis-NIR spectroscopy (Perkin Elmer Lambda 950) at wavelengths ranging from 300 nm to 1000 nm.

For transmission electron microscopy (TEM) analysis of CoO_x nanoparticles, a Phillips CM200 TEM operating at an accelerating voltage of 200 kV was used.

For the BPQDs, high-resolution TEM (HRTEM) images and diffraction patterns were acquired using an uncorrected FEI Titan Themis 80-200, at an accelerating voltage of 200kV. Energy-dispersive X-ray (EDX) analysis was carried out in TEM mode with the beam focused on the analysis region, using SuperX detectors and a low-background high-visibility holder.

X-ray diffraction (XRD) patterns were collected using PANalytical X'Pert Pro MPD with CoK_α radiation. 0.5° divergence slit was used before Parallel beam Goebel Mirror followed by a 1.4mm anti-scattering slit. Incident angle was kept at 1°. A 20mm height-limiting mask and 0.04 rad Soller slit controls beam width and divergence in axial direction. A 0.09° Equatorial Soller was used before a proportional counter on the secondary side. All data was scanned from 10 to 70 °2θ, with step size 0.05°, 1.5 s per step.

X-ray photoelectron spectroscopy (XPS) characterisation of the as-prepared CoO_x nanoparticles was performed on an ESCALab 250 Xi (Thermo Scientific) spectrometer with a monochromated Al K_α source. The pressure in the analysis chamber during measurement was $<10^8$ mbar. The pass energy and step size for narrow scans were 20 eV and 0.1 eV respectively, with a take-off angle normal to the sample surface. Spectral analysis was performed using Avantage 4.73 software and the curve fitting was carried out with a mixture of Gaussian–Lorentzian functions. *Kratos Axis Ultra* photoelectron spectrometer with a mono Al K_α (1486.6eV) x-rays was used for the XPS of the BPQDs.

Inductively Coupled Plasma-Mass Spectrometry (ICP-MS) was carried out using a Nexlon 300D-ICP-MS PerkinElmer instrument to gain information about the composition and weight percentage of the elements in the electrocatalysts. The carbon supported particles were digested in aqua-regia for 1 h at 80 °C to dissolve the phosphorus and cobalt, and then analysed at the selected "Co 59" and at "P 31".

The photoluminescence spectra were measured with a Horiba Jobin-Yvon Fluorolog 3 fluorimeter. The solution-based measurements were performed with the sample dissolved in **state solvent** and with photo-excitation at 330 nm, 360 nm, 390 nm and 420 nm. The slit width on the excitation and detection monochromator was varied to maximise the signal to noise with the measured spectra were corrected for the response of the instrument and normalised.

Electrochemical measurements

Electrochemical studies were carried out using a µAutolab potentiostat with three-electrode system including Pt-mesh electrode as the counter electrode and Hg|HgO|1 mol L^{-1} NaOH as the reference electrode. The working electrode was prepared by drop casting the electrocatalysts onto a glassy carbon RDE with 0.196 cm^2 area. The electrocatalytic activities were studied in the potential range from –0.20 to 1.80 V at 100 mV s^{-1} in 1 mol L^{-1} KOH as the electrolyte whilst rotating the working electrode at 1600 rpm. All potentials are reported against the reversible hydrogen electrode (RHE). The stability test was performed using a chronopotentiometry technique at a constant current density of 10.0 mA cm^{-2} for 2 h. The charge transfer resistance of the electrocatalysts was measured using an electrochemical impedance spectroscopy (EIS) at 1.609 V after electrochemical conditioning (5 cycles of CV) and fitted using Randles equivalent circuit and ZSimpWin software.

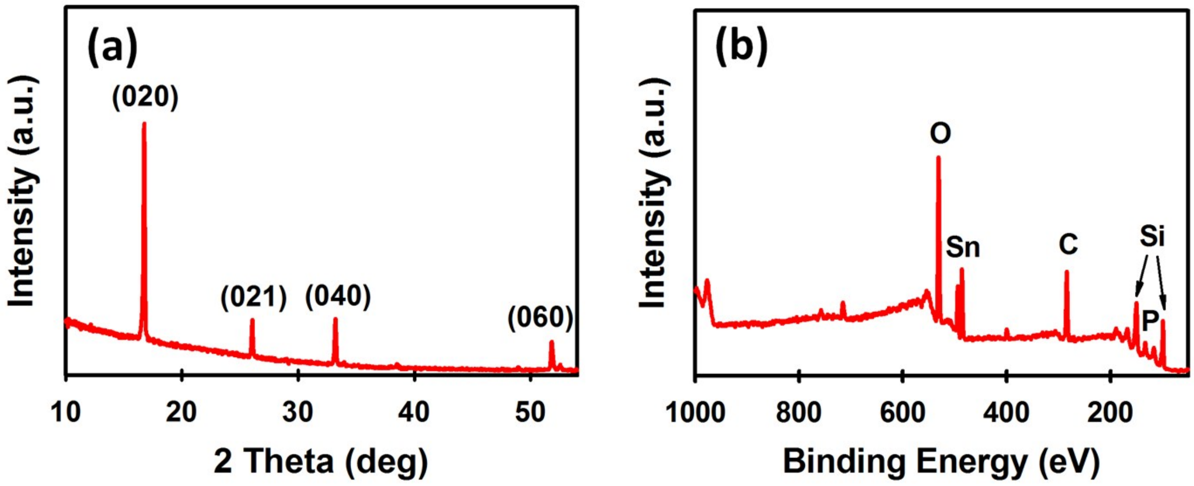

Fig. S1 (a) XRD pattern and (b) XPS survey spectrum of our BPQDs prepared using microwave-assisted method.

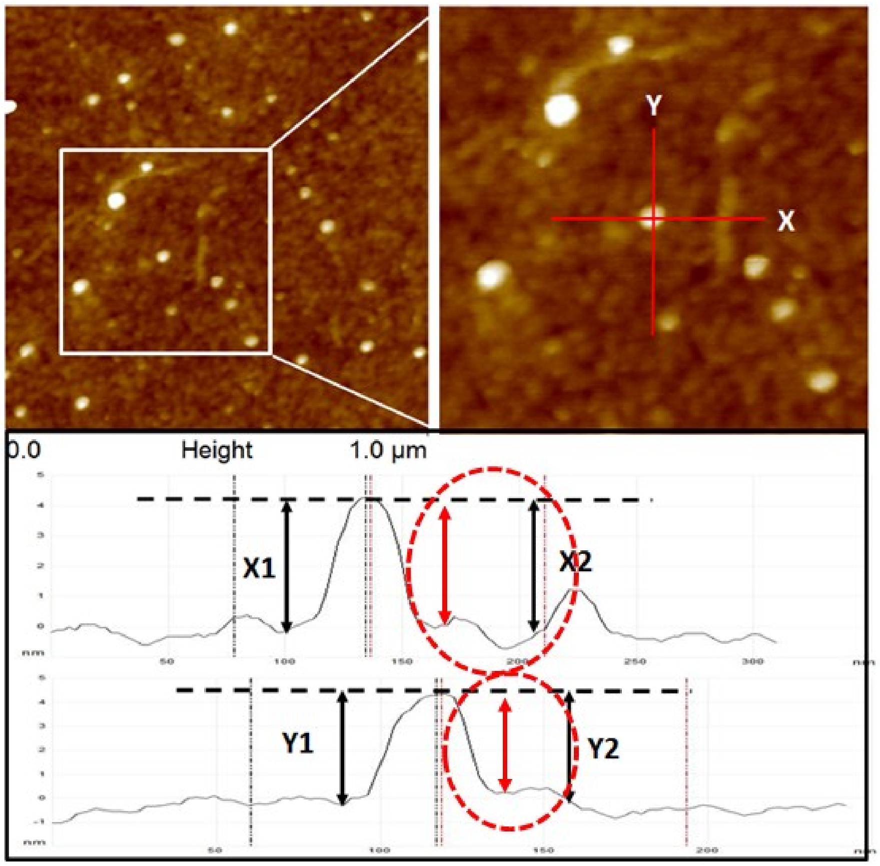

Fig. S2 AFM analysis of BPQDs.

Table S1. Height measurement of BPQDs from AFM images.

QD number	X1 (nm)	X2 (nm)	Y1(nm)	Y2(nm)	Average height (nm)
1	4.2	3.6	3.8	3.7	3.8
2	1.9	1.9	2.1	2.5	2.1
3	1.9	2.2	1.8	1.7	1.9
4	4.5	4.5	4.6	5.1	4.7
5	4.4	4	4.1	4.4	4.2
6	3	3	2.4	2.2	2.7
7	4.6	4.7	4.7	5	4.8
8	8.1	6.9	6.7	5.9	6.9
9	4.6	4.7	4.6	4.5	4.6
10	3.4	3.6	3.7	3	3.4
11	3.1	3.3	3.2	3.1	3.2
12	3.1	3.4	4.3	3.6	3.6
13	1.8	1.7	1.4	1.6	1.6
14	3.2	2.1	2.4	2	2.4
15	2.8	2.9	2.9	2.8	2.9
16	3.1	3.7	4	3.6	3.6
17	4.2	4.4	3.6	3.1	3.8
18	3.7	4.1	2.6	3	3.3
19	3.4	3.9	4	3.9	3.8
20	1.8	2	1.8	1.6	1.8
21	1.9	1.8	1.9	1.8	1.9
22	3.3	3.6	2.8	3.2	3.2
23	3.7	3.4	3.3	3.2	3.4
24	3.7	3.8	3.3	3.5	3.6
25	4.3	4	4.6	4.1	4.3
26	4.4	4.6	3.5	3.9	4.1
27	5.8	5.7	5.4	4.6	5.4
28	3.2	3	2.8	2.4	2.9
29	3.6	4.4	3.6	4.7	4.1
30	4.5	4.8	4.3	4.7	4.6
31	3.9	4	4	3.6	3.9
32	2.6	2.3	2.4	2.4	2.4
33	3.8	3.6	4.8	4.8	4.3
34	2.7	3.2	3.5	3.7	3.3
35	4	4.3	4.4	4.3	4.3
36	5.9	6	6	5.7	5.9
37	2.6	2.8	3.8	3.9	3.3
38	4.1	3.8	4.2	3.6	3.9
39	4.9	4.3	5	5.2	4.9
40	2.7	3.1	3.2	2.5	2.9

41	2.2	2.4	2.5	2	2.3
42	4.9	4.6	5.6	6	5.3
43	2.7	2.9	3.3	3	3.0
44	2.7	2.9	3	3.4	3.0
45	5.4	5.5	5.7	5.4	5.5
46	4.8	5.3	4.8	4.8	4.9
47	1.1	1.8	2.1	2.1	1.8
48	2.4	2.6	3.8	4	3.2
49	2.9	3.2	2.9	3.2	3.1
50	2	1.3	2.5	2.3	2.0
51	2.6	2.7	3.3	3.1	2.9
52	2.2	1.9	2.4	3	2.4
53	5	5	4.4	4.2	4.7
54	4.9	4.7	3.8	4.6	4.5
55	3.4	2.7	2.8	2.5	2.9
56	4.5	4.2	3.2	4.4	4.1
57	4.5	4.5	4.2	4.7	4.5
58	3.4	3.7	3.1	3.2	3.4

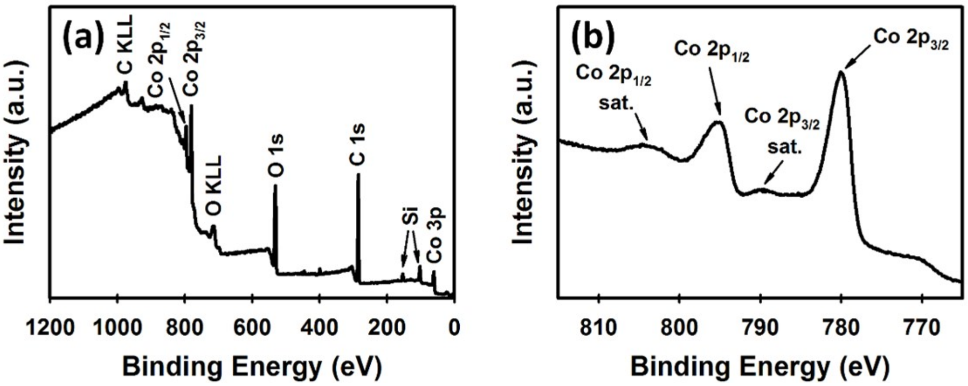

Fig. S3 (a) XPS survey spectrum and (b) high-resolution XPS spectrum of Co 2p of the as-prepared CoO_x nanoparticles.

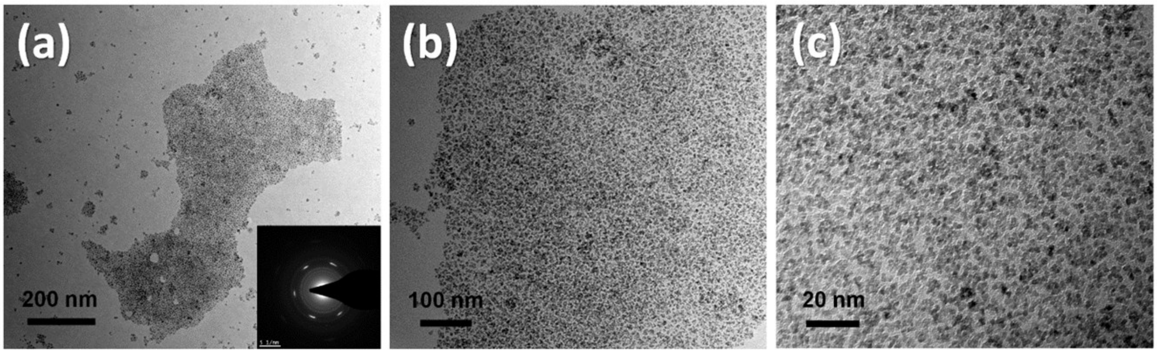

Fig. S4 TEM images of CoO_x nanoparticles.

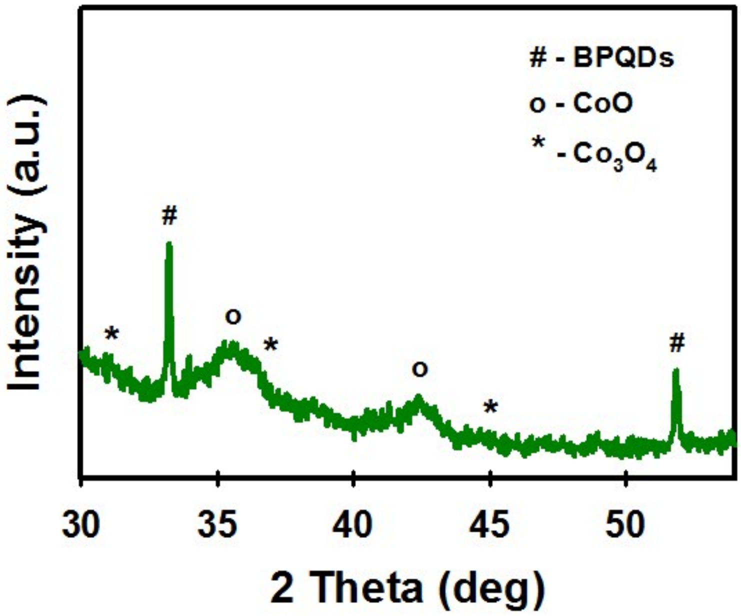

Fig. S5 XRD pattern of CoO_x/BPQDs composite.

Table S2. Comparison of catalytic performances of BP derivatives based electrocatalyst materials and commercial electrocatalysts (IrO_2, RuO_2) for OER.

Materials	Overpotential to reach 10 mA cm^{-2}	Electrolyte	Ref.
BPQDs	450 mV	1.0 M KOH	This work
FL-BP nanosheets	630 mV	1.0 M KOH	[3]
BP nanosheets	530 mV	1.0 M KOH	[4]
BPQDs	505 mV	1.0 M KOH	[5]
N-functionalised BPQDs	430 mV	1.0 M NaOH	[6]
S-doped BP nanosheets	410 mV	1.0 M KOH	[4]
CoO_x-BPQDs	360 mV	1.0 M KOH	This work
BP/Co_2P	380 mV	1.0 M KOH	[7]
BPQDs/MXene	360 mV	1.0 M KOH	[5]
IrO_2	330 mV	1.0 M KOH	[8]
RuO_2	320 mV	1.0 M KOH	[5]

Table S3. Mass percentage calculation from ICP-MS measurement.

	Content in carbon loaded sample, **wt %**			Concentration of the ink (2.5 mg/mL), **mg/mL**			Catalyst mass in film, **µg/20 µL**		
	Co	**P**	**C**	**Co**	**P**	**C**	**Co**	**P**	**C**
CoO_x/C	22.5	-	77.5	0.5625	-	1.9375	0.01125	-	0.03875
BP/C	-	1.9	98.1	-	0.0475	2.4525	-	0.00095	0.04905
CoO_x-BPQDs/C	22.2	1.5	76.3	0.555	0.0375	1.9075	0.0111	0.00075	0.03815

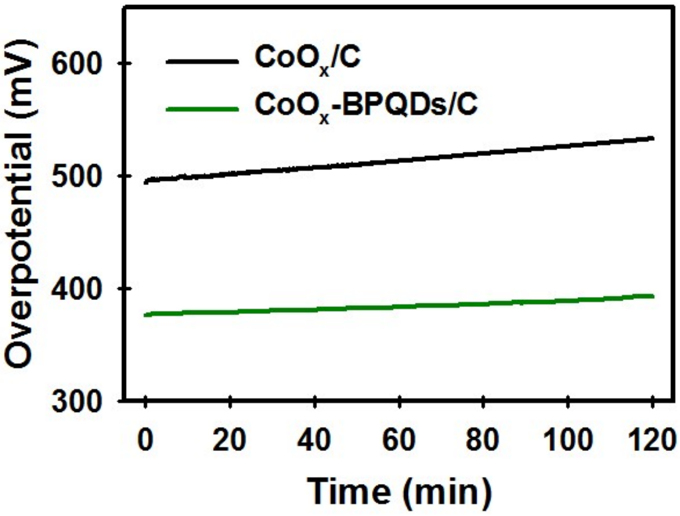

Fig. S6 Chronopotentiometric response at a constant current density of 10.0 mA cm^{-2} for CoO_x and CoO_x-BPQDs.

References

1. P. Nemes-Incze, Z. Osváth, K. Kamarás and L. P. Biró, *Carbon*, 2008, **46**, 1435-1442.
2. I. Calizo, A. A. Balandin, W. Bao, F. Miao and C. N. Lau, *Nano Lett.*, 2007, **7**, 2645-2649.
3. X. Ren, J. Zhou, X. Qi, Y. Liu, Z. Huang, Z. Li, Y. Ge, S. C. Dhanabalan, J. S. Ponraj, S. Wang, J. Zhong and H. Zhang, *Adv. Energy Mater.*, 2017, **7**, 1700396.
4. Y. Chang, A. Nie, S. Yuan, B. Wang, C. Mu, J. Xiang, B. Yang, L. Li, F. Wen and Z. Liu, *Nanotechnology*, 2018, **30**, 035701.
5. X.-D. Zhu, Y. Xie and Y.-T. Liu, *J. Mater. Chem. A.*, 2018, **6**, 21255-21260.
6. R. Prasannachandran, T. V. Vineesh, A. Anil, B. M. Krishna and M. M. Shaijumon, *ACS Nano*, 2018, **12**, 11511-11519.
7. J. Wang, D. Liu, H. Huang, N. Yang, B. Yu, M. Wen, X. Wang, P. K. Chu and X.-F. Yu, *Angew. Chem. Int. Ed.*, 2018, **57**, 2600-2604.
8. F. Song and X. Hu, *J. Am. Chem. Soc.*, 2014, **136**, 16481-16484.